Title: Polymer films containing chemically anchored diazonium salts with long-term stability as colorimetric sensors

Authors: Saúl E. Bustamante, Saúl Vallejos, Blanca Sol Pascual-Portal, Asunción Muñoz, Aránzazu Mendia, Bernabé L. Rivas, Félix C. García, José M. García

PII: S0304-3894(18)31095-1
DOI: https://doi.org/10.1016/j.jhazmat.2018.11.066
Reference: HAZMAT 19988

To appear in: *Journal of Hazardous Materials*

Received date: 30 May 2018
Revised date: 5 November 2018
Accepted date: 15 November 2018

Please cite this article as: Bustamante SE, Vallejos S, Pascual-Portal BS, Muñoz A, Mendia A, Rivas BL, García FC, García JM, Polymer films containing chemically anchored diazonium salts with long-term stability as colorimetric sensors, *Journal of Hazardous Materials* (2018), https://doi.org/10.1016/j.jhazmat.2018.11.066

Polymer films containing chemically anchored diazonium salts with long-term stability as colorimetric sensors

Saúl E. Bustamante,[b] Saúl Vallejos,[a,*] Blanca Sol Pascual-Portal,[a] Asunción Muñoz,[a] Aránzazu Mendia,[a] Bernabé L. Rivas,[b,*] Félix C. García,[a] José M. García[a,*]

[a] Departamento de Química, Facultad de Ciencias, Universidad de Burgos, Plaza de Misael Bañuelos s/n, 09001 Burgos, Spain. Fax: (+) 34 947 258 831, Tel: (+) 34 947 258 085. Email: jmiguel@ubu.es (JMG), svallejos@ubu.es (SV)

[b] Polymer Department, Faculty of Chemistry, University of Concepción, Casilla 160-C, Concepción, Chile. Fax: +56 41 2245974; Phone: +56 41 2203373. Email: brivas@udec.cl (BLR)

Graphical Abstract

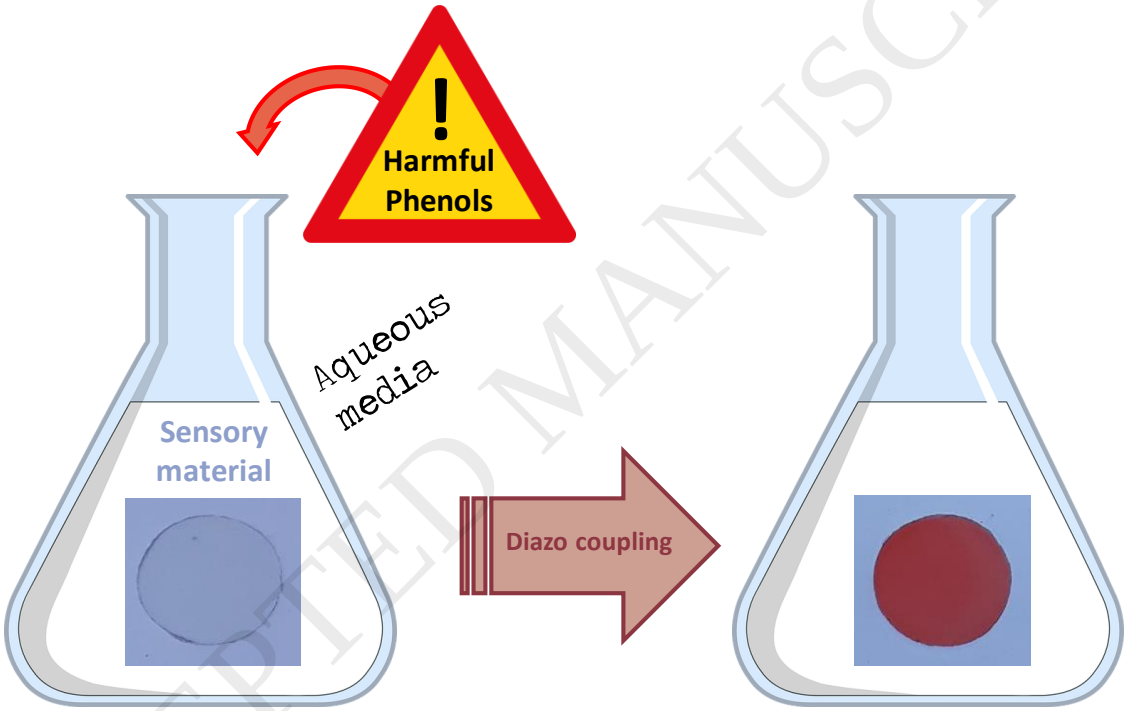

Highlights

- Film shaped sensory polymeric materials change their color in presence of phenols
- The polymers main chains have pendant diazonium moieties
- The sensory materials are manageable and stable along time
- The detection is achieved visually and also using pictures taken with smartphones
- The limits of detection were of the order of ppb

Abstract

We have prepared polymeric films as easy-to-handle sensory materials for the colorimetric detection and quantification of phenol derivatives (phenols) in water. Phenols in water resources result from their presence in pesticides and fungicides, among other goods, and are harmful ecotoxins. Colorless polymeric films with pendant diazonium groups attached to the acrylic polymer structure were designed and

prepared for use as sensory matrices to detect phenol-derived species in water. Upon dipping the sensory films into aqueous media, the material swells, and if phenols are present, they react with the diazonium groups of the polymer to render a highly colored azo group, giving rise to the recognition phenomenon. The color development can be visually followed for a qualitative determination of phenols. Additionally, quantitative analysis can be performed by two different techniques: a) by using a UV-Vis spectrophotometer (limit of detection of 0.12 ppm for 2-phenylphenol) and/or b) by using a smartphone with subsequent RGB analysis (limit of detection of 30 ppb for 2-phenylphenol).

Keywords: Polymeric sensors; film shaped sensors; colorimetric sensors; phenol sensors

Introduction

Phenols are harmful ecotoxins with both natural [1] and anthropogenic origins. They are mutagenic and carcinogenic products, exhibit hepato- and hematotoxic activity toward all kinds of living beings, and their elimination through oxidation and/or degradation processes has been widely studied [2-6]. From a human activity viewpoint, environmental pollution related to phenol derivatives comes from the petrochemical, chemical and pharmaceutical industries that produce goods in which phenols are used, such as drugs, household chemicals, dyes, and polymers. In particular, the presence of phenols in the ecosystem is worryingly related to the use and degradation of pesticides and biocides (the germicidal activity of phenol was discovered in 1865 by Joseph Lister). Among all kinds of phenolic products, the most widespread are chlorophenols, formed from the chlorination of mono- and polyaromatic phenols present in the water and soil. Other relevant phenol-derived families are nitrophenols, alkylphenols, bisphenols and aminophenols [7-9].

Currently, phenols in the environment are detected by GC/MS (gas chromatography coupled with mass spectrometry) or HPLC (high-performance liquid chromatography) coupled to different detectors [10]. These techniques require, in addition to expensive instrumentation and trained personnel, laborious and time-consuming microextraction steps (SPME or LPME) [11,12]. Additionally, biosensors have been proposed [12,13], along with a number of electrochemical methods [14-16], including the use of quantum dots [17]. Systems based on colorimetric or fluorimetric detection of different contaminants are a good alternative to these conventional methods [18-24].

We propose the in situ visual detection and quantification of phenols in aqueous media by untrained personnel by using inexpensive and rapid colorimetric sensory films. These sensory films are acrylic polymers with stable diazonium salts chemically anchored to the polymeric structure. The films swell in water, where the phenols penetrate by diffusion before undergoing azo coupling with the diazonium salts to give the strongly colored azo compounds. The azo coupling reaction is the well-known basis for the preparation of synthetic azo dyes, which have been intensively used since the third quarter of the 19th century [25-28]. In this regard, the noteworthy stability under laboratory temperature and light conditions of polymer materials with diazonium groups should be mentioned compared to that of the discrete benzenediazonium chloride derivatives, which are an interesting chemical species used in the preparation of a number of chemicals that decompose above 5 °C and, accordingly, are prepared in ice-cold solutions and used immediately, without isolation.

EXPERIMENTAL

Materials

All materials and solvents were commercially available and used as received unless otherwise indicated. The following materials and solvents were used: sodium hydroxide (VWR, 99%), 2,2'-azobis(2-methylpropionitrile) (AIBN) (Aldrich, 98%), 1-vinyl-2-pyrrolidone (VP) (Aldrich, 99%), methylmethacrylate (MMA) (Aldrich, 99%), 4-aminostyrene (Aldrich, 99%), sodium nitrite (VWR, 99.5%), *m*-cresol (Alfa Aesar, >99%), 2-chlorophenol (Alfa Aesar, >99%), bisphenol-A (Acros Organics, >97%), 2-nitrophenol (Alfa Aesar, >98%), 2,4-dinitrophenol (Alfa Aesar, >96%), fenhexamid (Aldrich, 99%), 2,4-dichlorophenol (Alfa Aesar, >99%), 4-chlorophenol (Alfa Aesar, >99%), 4-chloro-2-methylphenol (Aldrich, 97%), 2,4-dimethylphenol (Aldrich, 98%), 2-phenylphenol (Aldrich, 99%), 1-naphthol (Aldrich, >99%), and 1,8-dihydroxyanthraquinone (Aldrich, 96%).

In the tests carried out with the product, the commercial pesticide DECCO® OPP and a fungicide widely used for postharvest treatment of fungi causing rot (*Penicillium* spp, *Rhizopus* spp), mainly in citrus fruits, were used. This pesticide is formulated as an emulsifiable concentrate and contains as an active component 2-phenylphenol (concentration: 10% w/v (100 g/L)), in addition to other elements in very low concentrations such as Si (15080.5 ppb), Mn (1.8 ppb), Zn (622.3 ppb), Pd (49.4 ppb) and Ba (7.2 ppb).

Measurements and instrumentation

The optical analysis was carried out by taking digital pictures of the sensory films with a smartphone Samsung J7 prime after immersion in aqueous media with different concentrations of phenols. This procedure allowed for the quantification of each phenol concentration using the "B" (blue) and the "R" (red) parameters of the RGB (red, green and blue) color model [29,30]. The "B" and "R" color parameters for each disc were obtained immediately after taking the pictures with the smartphone using the ColorMeter app to automatically average the data over an 11 X 11 (121) pixel area. Due to the possible influence of ambient light on the image quality, a homemade retro-illumination box was used, which allowed good repeatability for the imaging analysis [30]. In addition, the UV-Vis spectra were recorded using a U-3900 UV/Vis spectrophotometer.

The starting materials were thermally and mechanically characterized using thermogravimetric analysis (TGA, 10-15 mg of sample under a synthetic air and nitrogen atmosphere with a TA Instruments Q50 TGA analyzer at 10 °C min^{-1}), differential scanning calorimetry (DSC, 10-15 mg of sample under nitrogen atmosphere with a TA Instruments Q200 DSC analyzer at 20 °C min^{-1}), and tensile properties analysis (5 x 9.44 x 0.122 mm samples using a Shimadzu EZ Test Compact Table-Top Universal Tester at 1 mm min^{-1}).

The infrared spectra of the sensor films were recorded using a synchrotron light beam coming from a particle accelerator (ALBA synchrotron, Barcelona-Spain), utilizing the FTIRM (Fourier transform infrared microspectroscopy) technique in transmission mode, employing a Hyperion 3000 microscope coupled to the Vertex 70 spectrometer (Bruker, Germany, 4000-400 cm^{-1}). High-resolution electron-impact mass spectrometry (EI-HRMS) was carried out on a Micromass AutoSpect Waters mass spectrometer (ionization energy: 70 eV; mass resolving power: >10000). The ^{1}H and ^{13}C NMR spectra were recorded with a Varian Inova 400 spectrometer operating at 399.92 and 100.57 MHz, respectively, with deuterated dimethyl sulfoxide as the solvent.

The weight percentage of water taken up by the films upon soaking in pure water at 20 °C until reaching equilibrium (water-swelling percentage, WSP) was obtained from the weight of a dry sample film (ω_d) and its water-swelled weight (ω_s) using the following expression: $WSP = 100 \times [(\omega_s - \omega_d)/\omega_d]$.

Polymer synthesis

The starting material was obtained by radical copolymerization of the different monomers: vinylpyrrolidone (**VP**) as the hydrophilic monomer, methylmethacrylate (**MMA**) as the hydrophobic monomer, and 4-aminostyrene (**SNH_2**) as the anchorage monomer. The bulk radical polymerization was carried out in a silanized glass mold (100 μm thick) in an oxygen-free atmosphere at 60 °C overnight. In regard to the molar ratio of the monomers, this can be adjusted for different purposes. In our case, the colorimetric response of the material toward phenols was modulated by adjusting this molar ratio, i.e., 49.975/49.975/0.05 (**VP**/**MMA**/**SNH_2**) (**F_{005}**, for preparing sensory films for sensing phenols that produce strong colors upon interaction with the sensory film), 49.875/49.875/0.25 (**VP**/**MMA**/**SNH_2**) (**F_{025}**, for preparing sensing films for detecting phenols that produce soft colors upon interaction with the sensory film), and 45/45/10 (**VP**/**MMA**/**SNH_2**) (**F_{10}**, for FT-IR characterization. The high molar content of **SNH_2** allows for following by infrared spectroscopy both the preparation of the sensory material and the sensing mechanism). The chemical structure of the films used to prepare the sensory materials is depicted in Scheme 1. Additionally, the thermally initiated bulk polymerization procedure for polymers prepared with VP results in crosslinked materials [31], which limits conventional NMR or GPC analysis. Thus, we have prepared a linear polymer with the same monomer feed ratio. The ^{1}H NMR analysis of the linear polymer, which is soluble, confirms that the structural units conforming the polymers structure corresponds with the ratio of monomers used to prepare the macromolecule. The synthesis and characterization of the linear polymer is showed in ESI, Section S4.

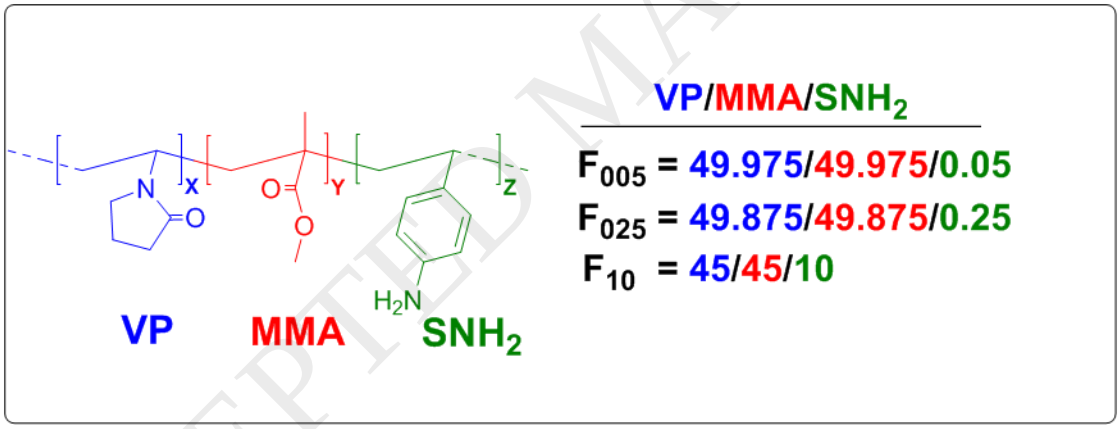

Scheme 1 Chemical structure of the polymer films.

The sensory materials were prepared from the films **F_{005}**, **F_{025}** or **F_{10}** with a solid-state reaction by dipping 8 mm discs of these films into 10 mL of an aqueous solution containing 1 mL of HCl (37%) and 40 mg of $NaNO_2$ at RT for 90 min (see Scheme 2). In this way, materials with pendant benzenediazonium salt motifs (**F_{005}B, F_{025}B** and **F_{10}B**) were readily prepared.

RESULTS AND DISCUSSION

The reactions between phenols and diazonium salts in basic aqueous media have been studied for decades [32,33]. These reactions give rise to highly colored products that are commonly used in the pigments and dyes industry.

In this work, we prepared polymeric film materials from two main commercially available comonomers (**VP**, **MMA**) and a third comonomer (**SNH_2**), added in small ratios to the others, which acts

as an anchorage monomer providing pendant aniline groups to the polymeric structure. The main comonomers (**VP**, hydrophilic; **MMA**, hydrophobic) provide the polymer films with the correct hydrophilicity balance needed for sensory purposes in aqueous media, i.e., the ability to swell in water without losing mechanical behavior in the swollen state [34,35].

As shown in Scheme 2, the amine groups of the aniline moieties react with sodium nitrite in acidic aqueous media to produce the sensory materials, with pendant benzenediazonium groups (**F_{005}B, F_{025}B** and **F_{10}B**). These colorless materials are stable for weeks and are capable of detecting phenols in basic aqueous media, with low limits of detection (**LOD**) and quantification (**LOQ**), by the reaction of the benzenediazonium groups with the target phenols to produce colored films, where the colors come from the formation of pendant azo groups (**F_{005}C, F_{025}C** and **F_{10}C**). This chemical reaction is intrinsically non-reversible; thus, the sensor is actually a chemical dosimeter.

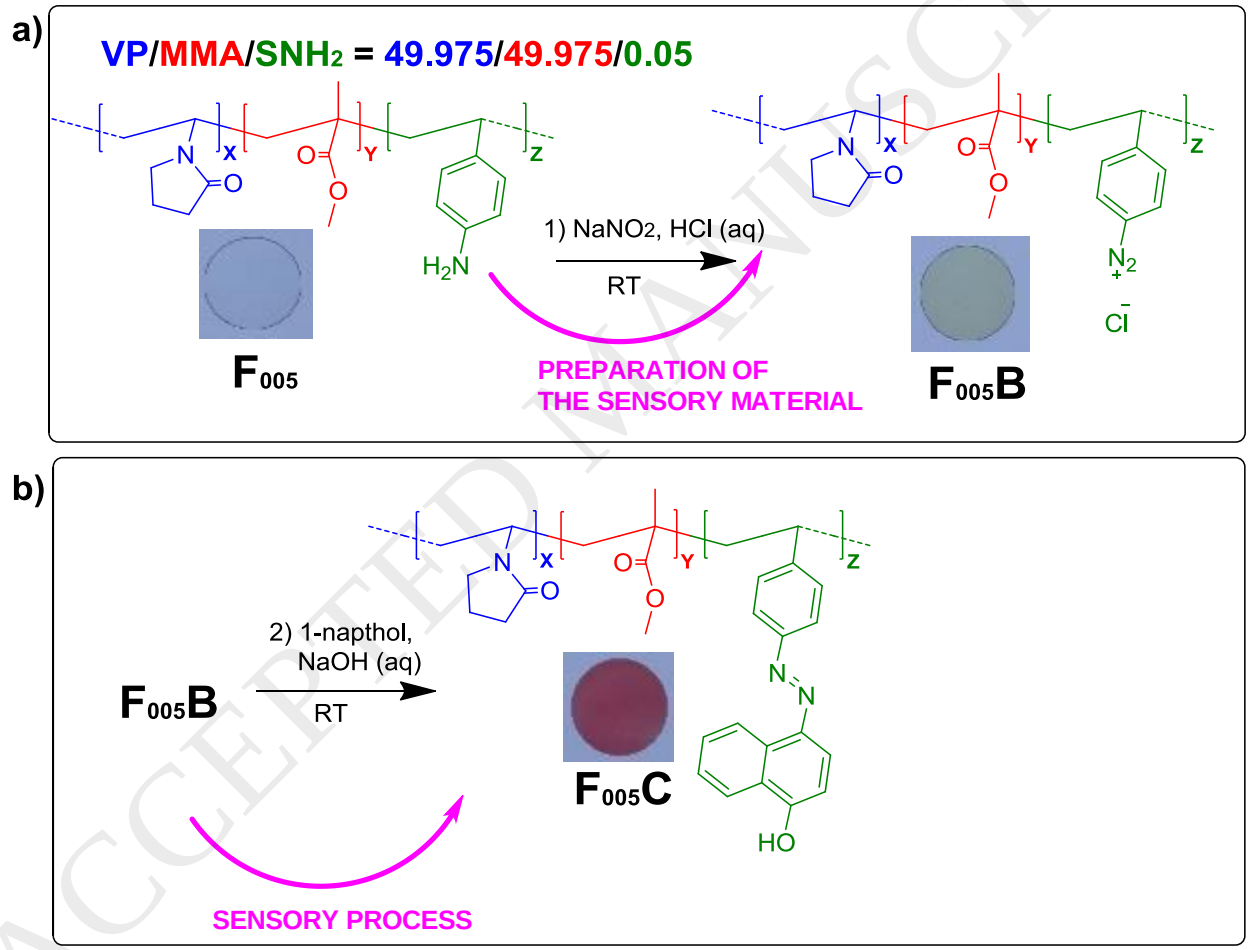

Scheme 2. Example of the preparation of the sensory films (a) by dipping an 8 mm disc of the film into 10 mL of an aqueous solution containing 1 mL of HCl (37%) and 40 mg of $NaNO_2$ at RT for 90 min, and (b) example of the sensing process for 1-naphthol carried out by dipping the sensory film into 10 mL of an aqueous solution containing 40 mg of NaOH and 130 mg of 1-naphthol.

Water uptake

Usually known as the water swelling percentage (**WSP**) [33,34], water uptake is a critical parameter for these kinds of materials and is intimately related to both the manageability properties and the transport

of water soluble target species into the swelled sensory materials, where the chemical reactions that give rise to sensing take place. Thus, the higher the water uptake is, the higher the transport rate and, at the same time, the worse the manageability properties. Thus, it is very important to achieve the best balance between both properties. For this application, **F_{005}**, **F_{025}**, and **F_{10}** exhibited WSPs of 64%, 54% and 20%, respectively, with good manageability in the water-swollen state and rapid response of the sensory materials derived from them, especially **F_{005}** and **F_{025}**.

Thermal and mechanical analysis

The thermogravimetric analysis (TGA) of the materials was carried out under an inert (nitrogen) atmosphere at a scan rate of 10 °C min^{-1} by measuring samples of 10–15 mg of film for **F_{005}**, **F_{025}** and **F_{10}**. The data for the 5% (T_5) and 10% (T_{10}) weight loss under nitrogen atmosphere were (T_5/ T_{10}) 353 ^{o}C/364 ^{o}C, 353 ^{o}C/366 ^{o}C, and 311 ^{o}C/370 ^{o}C, respectively. The T_5 of **F_{10}** is significantly lower due to the high content of aniline moieties derived from the **SNH_2** monomer, as is graphically depicted in the ESI, Section S1.

The glass transition temperatures (Tg) of the materials were calculated by DSC analysis at 20 ^{o}C min^{-1}, obtaining values for **F_{005}**, **F_{025}** and **F_{10}** at approximately 140 ^{o}C, i.e., the content of **SNH_2** does not meaningfully influence the Tg.

The Young´s modulus values for **F_{005}**, **F_{025}** and **F_{10}** were obtained by mechanical analysis of 10 strips of each material (5 mm width, 30 mm length, and 100−120 μm thick) after drying at 60 ^{o}C for 1 h. The speed of the method was 5 mm min^{-1}, with a gauge length of 10 mm. Higher molar ratios of **SNH_2** increased the Young´s modulus, obtaining values for **F_{005}**, **F_{025}**, and **F_{10}** of 494, 566, and 873 MPa, respectively.

Response time

The prepared materials are intended to be used as sensors in real-world applications; thus, the response times must be as low as possible. We have studied the response times of a number of sensory films in previous works [30,33,36], and this parameter depends on multiple variables, such as the thickness of the films, the molar ratio of the sensory motifs, and the hydrophilicity of the material. For example, the higher the molar ratio of the sensory motif is, the lower the response time, and complementarily, the higher the **WSP** is, the lower the response time. In this case, we worked with 100 μm thickness films with a **WSP** between 20 and 60%, depending on the molar ratio of the sensory motif provided by films prepared from 0.05 to 10%. The response times for **F_{005}B**, **F_{025}B**, and **F_{10}B** are 120, 5, and 3 min, respectively (additional information in the ESI, Section S2). Considering the economic aspects related to the use of widely available commercial comonomers (**VP** and **MMA**), the optimal material for this application is **F_{025}B**. Table 1 shows the figures of merit for comparing the performance of this sensory material with other techniques and methods for the detection of phenols.

Stability of the sensory materials

To study the stability of the formed diazonium salt moieties within the material, we prepared 60 discs of **F_{005}B** (8 mm diameter) and kept them wet (water swollen) in commercial zipper storage bags at room temperature and without special care (without protecting from light). To test the performance of the material as a phenol sensor over time, three discs were dipped into 10 mL of an aqueous solution of NaOH (0.1 M) and 1-naphthol (0.01 M) for 1 h at different times (up to 13 days). The discs were thoroughly washed with an aqueous solution of 0.1 M NaOH before taking a photograph with a smartphone to study its color. The results of the three discs tested at each timepoint were averaged. The response of the material was virtually the same over the testing period (13 days), as shown in Figure 1. Accordingly, the benzenediazonium salt motifs are stable within the material, and this result is noteworthy because these types of salts are considered inherently unstable and used without isolation in conventional organic chemistry.

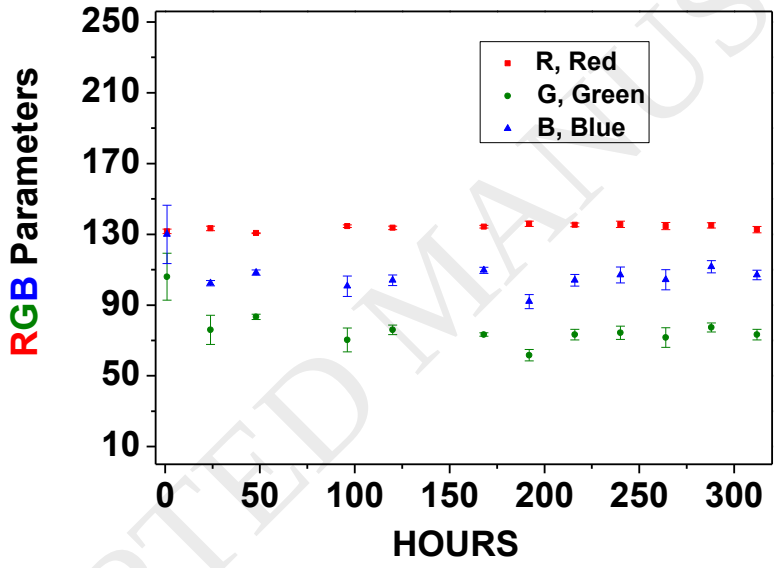

Figure 1. R (red), G (green), and B (blue) parameters defining the digital color of the film, **F_{005}B,** after storage for different amounts of time and then submergence in an aqueous solution of phenols. The stored 8 mm discs of **F_{005}B** were dipped in 10 mL of aqueous solution of NaOH (0.1 M) and 1-naphthol (0.01 M). The pictures were taken with a conventional smartphone and the RGB parameters defining the color of each film were measured.

Characterization of the solid-state reaction

Infrared spectra were collected using synchrotron radiation on 10 μm thick films of **F_{10}** and **F_{10}C (1-naphthol),** obtained from the interaction of **F_{10}** with 1-naphthol. The band observed between 20050 and 2300 cm^{-1} in **F_{10}B** corresponds with the stretching of N≡N, whereas the observed band centered at 1576 cm^{-1} in the **F_{10}C (1-naphthol)** spectrum confirms the formation of the diazo compound (see Figure 2).

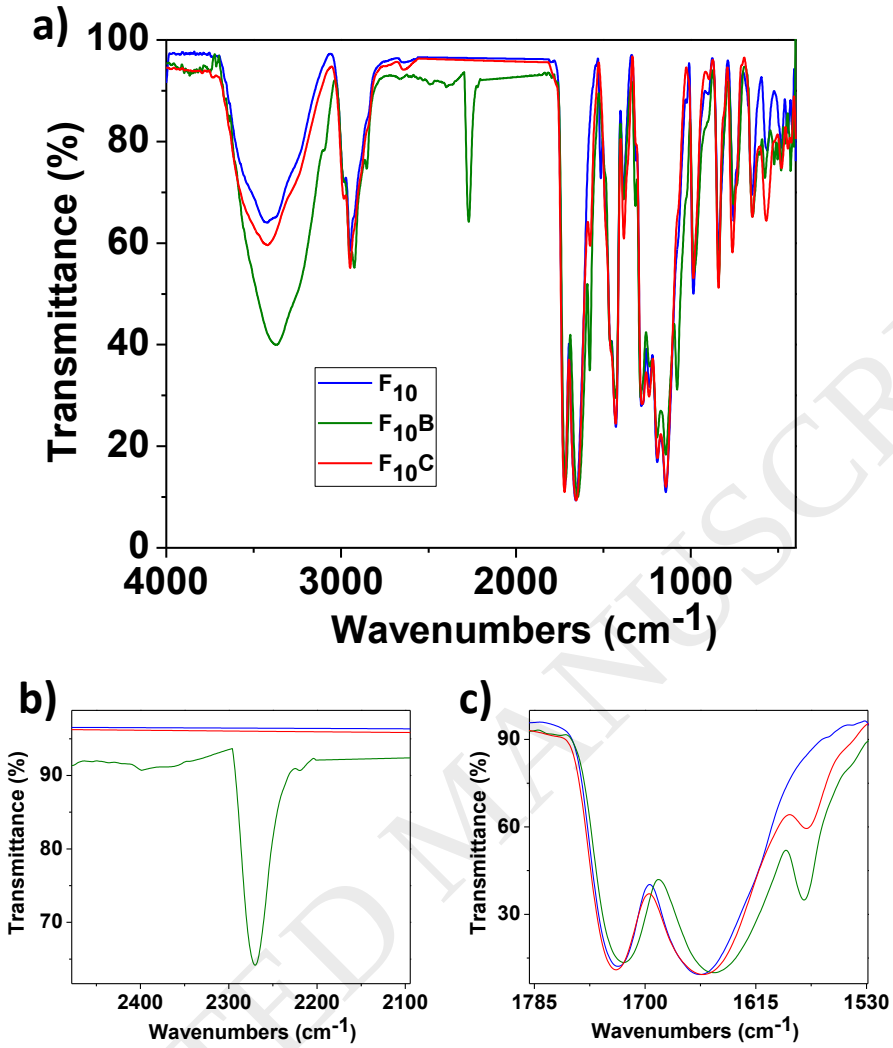

Figure 2. a) FT-IR spectra of the sensory materials **F_{10}**, **F_{10}B** and **F_{10}C (1-naphthol);** b) Expansion of interesting regions.

Additionally, we prepared and characterized a model compound from *p*-toluidine and 1-naphthol under the same conditions, obtaining high yield and purity. The chemical characterization of the model is described in the ESI, Section S3. To further study the material, we performed various SEM measurements on the surface of the films, but we did not find remarkable results due to the dense nature of the films.

Phenol detection performance

We decided to test the performance of the sensory materials using 13 of the most common harmful phenols in pesticides, fungicides and other applications (see Table 2).

Thus, aqueous solutions (NaOH 0.1 M) of each phenol at different concentrations were prepared. Discs (8 mm diameter) of **F_{005}B** were dipped into 10 mL of each phenol solution at room temperature for 60 min. After that, the discs were thoroughly washed with aqueous NaOH (0.1 M) and photographed with a smartphone, and their UV-Vis was recorded. Figure 3 shows, as an illustrative example, the results for sensing 1-naphthol. Note that preliminary interference tests with metal cations and organic/inorganic anions were performed as depicted in previous work [30], and no relevant results were observed.

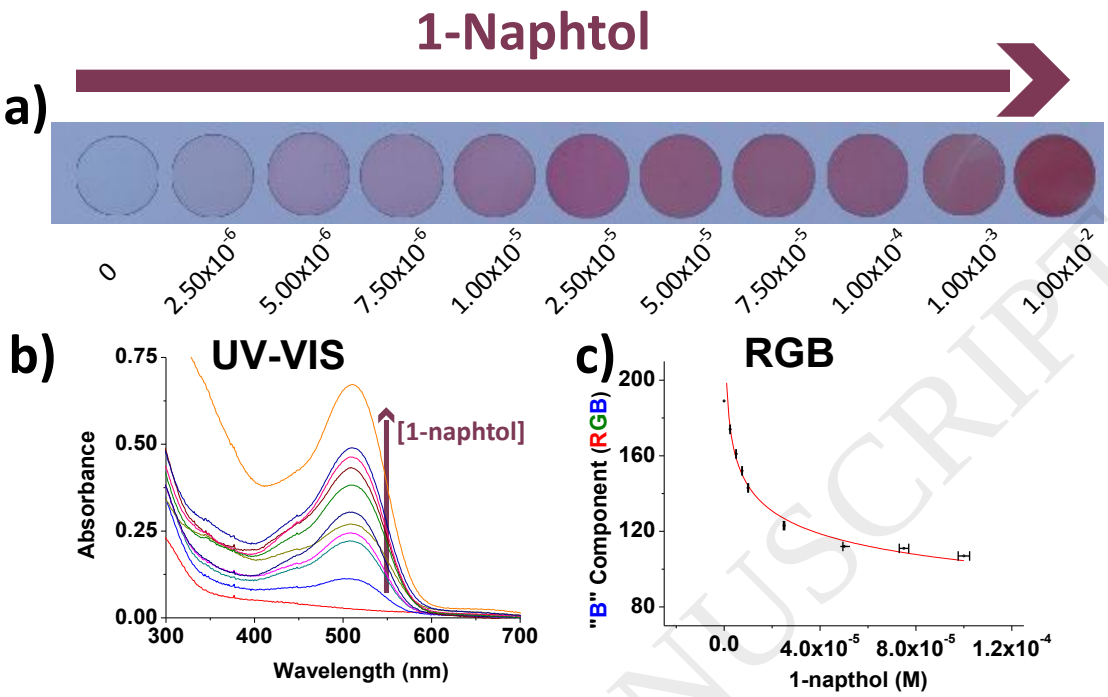

Figure 3. a) Digital photograph of F_{005} discs after immersion for 60 min at RT in aqueous solutions (NaOH 0.1 M) containing concentrations of 1-naphthol between $2.5x10^{-6}$ and $1.00x10^{-2}$ M; **b)** UV-Vis spectra obtained from the discs (LOD and LOQ of $8.44x10^{-7}$ M and $2.57x10^{-6}$ M, respectively); **c)** titration curve for the blue component (RGB) of the discs (LOD and LOQ of $1.25x10^{-6}$ M and $3.80x10^{-6}$ M, respectively; the blue component is not sensitive to higher concentrations of 1-naphthol, which are neither depicted nor used in the curve fitting).

Figure 4 shows the colorimetric response of sensory materials for the analyzed phenols. When the colorimetric response was not clearly visible with **F_{005}B**, a material with a higher concentration of the sensory motifs was used (**F_{025}B**).

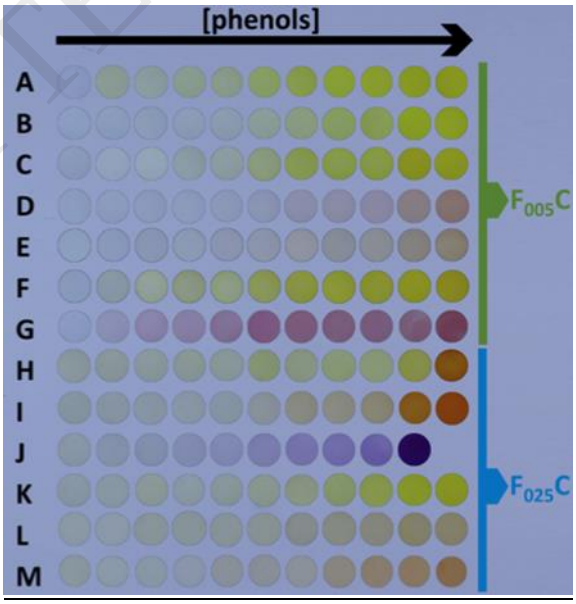

Figure 4. Color matrix of sensory discs after being in contact with phenols in water. A set of vials with solutions of aqueous 0.1 M NaOH and varying phenol concentrations was freshly prepared, and one disc (8 mm diameter) of $\mathbf{F_{005}B}$ or $\mathbf{F_{025}B}$ was dipped into each solution for 60 min at RT. The UV-Vis spectra and RGB parameters of each sensory disc were obtained (see the ESI, Section S6). $\mathbf{F_{005}B}$ discs were dipped into solutions with phenol concentrations ranging from $2.5x10^{-6}$ M to $1x10^{-2}$ M to obtain $\mathbf{F_{005}C}$ discs: (**A**) *m*-cresol, (**B**) 2-chlorophenol, (**C**) bisphenol-A, (**D**) 4-chloro-2-methylphenol, (**E**) 2,4-dimethylphenol, (**F**) 2-phenylphenol and (**G**) 1-naphthol. $\mathbf{F_{025}B}$ discs were dipped into solutions with phenol concentrations ranging from $2.5x10^{-6}$ M to $1x10^{-2}$ M to obtain $\mathbf{F_{025}C}$ discs: (**H**) 2,4-dinitrophenol, (**I**) 4-chlorophenol and (**J**) 1,8-dihydroxyanthraquinone. $\mathbf{F_{025}B}$ discs were dipped into solutions with phenols concentration ranging from $1x10^{-5}$ M to $1x10^{-2}$ M to obtain $\mathbf{F_{025}C}$ discs: (**K**) 2-nitrophenol, (**L**) fenhexamid and (**M**) 2,4-dichlorophenol.

A summary of the performance of each sensory material in terms of the LOD and LOQ for each studied phenol is shown in Table 3 (additionally, the individual RGB and UV-Vis data and analysis of each phenol is shown in the ESI, Section S6).

Application to a commercial product

After the analysis of the performance of the sensory materials for sensing phenols in water, we carried out a test with a commercial product, specifically, a fungicide based on 2-phenylphenol. In the data sheet of the product (ESI, Section S5), the manufacturer specifies that the product contains 100 g of 2-phenylphenol per liter (0.5875 M). Therefore, we diluted the sample to reach a concentration of $4x10^{-5}$ M with aqueous 0.1 M NaOH prepared with tap water. Then, one 8 mm diameter disc of $\mathbf{F_{005}B}$ was dipped in 10 mL of this solution at room temperature for 60 min. Then, the film was thoroughly washed with aqueous 0.1 M NaOH and photographed with a smartphone. The "B" parameter (RGB parameter) obtained from the photograph was used to calculate the concentration of 2-phenylphenol in the commercial product, DECCO® OPP 20 using the equation obtained from the titration of 2-phenylphenol (ESI, Section S6 (K)). Figure 5 shows the result of the calculated concentration of 2-phenylphenol, which is in agreement with the concentration provided by the manufacturer.

Additionally, we have checked the stability of the material dipped in DECCO (see ESI, Section S2-d), by dipping one disk of $\mathbf{F_{005}B}$ in DECCO and registering the absorbance at 464 nm each minute during 5 days, and the material remains stable once reached the equilibrium of the system.

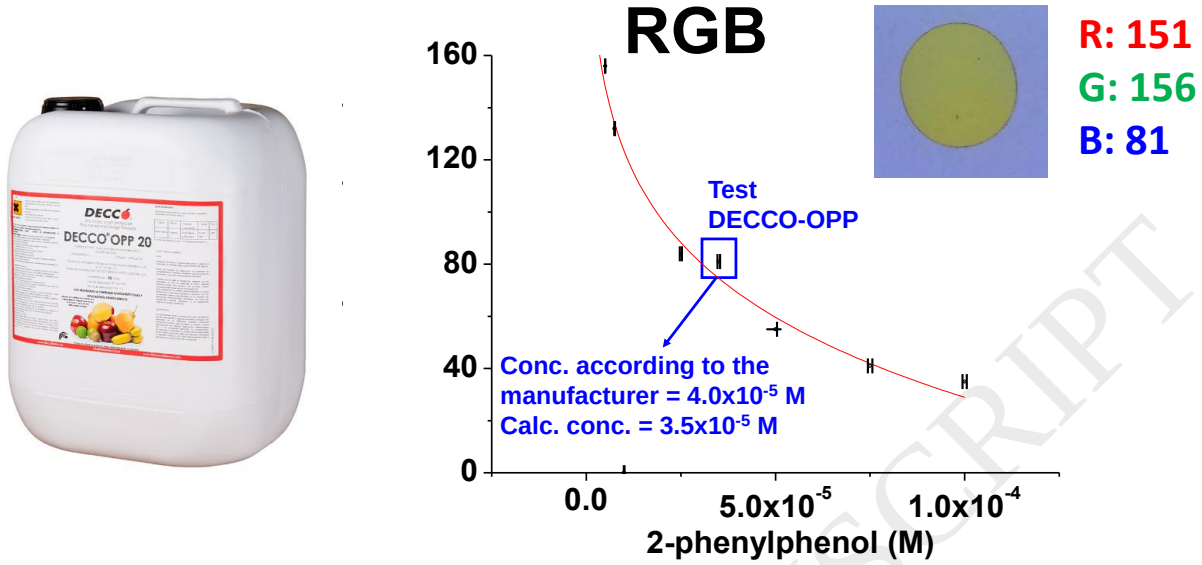

Figure 5 Left: Image of the container of the tested commercial product. Right: titration curve using the analysis of pictures taken of the sensory discs (B parameter). The concentration of 2-phenylphenol in the commercial product was calculated using the titration curve (logarithmic fitting).

Interference study

ICP-MS analysis of a prepared sample of 2-phenylphenol (0.58 M in aqueous 0.1 M NaOH) and the commercial product (DECCO® OPP) was carried out. The results are shown in Table 4.

As described previously, the concentration of 2-phenylphenol within the commercial product, DECCO® OPP, was correctly calculated using the titration curve obtained from the color of the sensory films of **F_{005}B** after dipping into a lab-made solution of 2-phenylphenol. Thus, no interference of the different elements found in the commercial product was observed.

Conclusions

We prepared polymer films with diazonium moieties pendant to the main acrylic chains. The diazonium groups within the solid materials are stable over time and can be handled without special care by untrained personnel. The materials have a gel-like behavior, and swell upon dipping in water. The colorless films react with any phenol present in the water, developing color, due to the formation of azo groups, which we have used to visually signal the presence of phenols. Additionally, we have titrated the phenols using both a conventional analytical technique, UV-Vis, and an analysis of the colors of pictures taken of the sensory films with a handheld device (e.g., a smartphone); detection limits ranged from ppb to ppm. In short, we have used a well-known organic reaction for sensory purposes. To achieve this objective, we prepared materials with chemical groups considered inherently unstable under ambient conditions, exploiting the solid-state chemistry within a macromolecular environment that usually exhibits completely different chemical behavior both in solution and for low molecular mass species.

Acknowledgements

The financial support provided by Fondo Europeo de Desarrollo Regional (FEDER) and both the Spanish Agencia Estatal de Investigación (AEI) (MAT2017-84501-R) and the Consejería de Educación – Junta de Castilla y León (BU061U16) is gratefully acknowledged. We also thank the "ALBA Synchrotron", belonging to the network of "Infraestructura Científico y Técnica Singular (ICTS)", Spain, for the project Nº 2017022034, titled "Structural data by infrared microspectroscopy in inorganic-organic hybrid polymer materials in the form of films with interesting optical-, antitumor-, bactericide- or sensing properties".

References

[1] H. Swarts, F. Verhagen, J. Field, J. Wijnberg, Trichlorinated phenols from hypholoma elongatum, Phytochemistry 49 (1998) 203-206.

[2] M. Pirsaheb, S. Moradi, M. Shahlaei, N. Farhadian, Application of carbon dots as efficient catalyst for the green oxidation of phenol: Kinetic study of the degradation and optimization using response surface methodology, J. Hazard. Mater. 353 (2018) 444– 453.

[3] H. Wang, M. Jing, Y. Wu, W. Chen, Y. Ran, Effective degradation of phenol via Fenton reaction over CuNiFe layered double hydroxides, J. Hazard. Mater. 353 (2018) 53– 61.

[4] J. Gao, Y. Liu, X. Xia, L. Wang, W. Donga, Fe1-xZnxS ternary solid solution as an efficient Fenton-like catalyst for ultrafast degradation of phenol, J. Hazard. Mater. 353 (2018) 393– 400.

[5] H. Wang, Y. Liang, L. Liu, J. Hu, W. Cui, Highly ordered TiO2 nanotube arrays wrapped with g-C3N4 nanoparticles for efficient charge separation and increased photoelectrocatalytic degradation of phenol, J. Hazard. Mater. 344 (2018) 369– 380.

[6] H. Zhou, G. Wang, M. Wu, W. Xu, X. Zhang, L. Liu, Phenol removal performance and microbial community shift during pH shock in a moving bed biofilm reactor (MBBR), J. Hazard. Mater. 351 (2018) 71– 79.

[7] J. Michałowicz, W. Duda, Carbon black as low-cost alternative for electrochemical sensing of phenolic compounds, Pol. J. Environ. Stud. 16 (2007) 347-362.

[8] G. Busca, S. Berardinelli, C, Resini, L, Arrighi, Technologies for the removal of phenol from fluid streams: A short review of recent developments, J. Hazard. Mater. 160 (2008) 265–288.

[9] Toxicological Review of Phenol, EPA/635/R-02/006, U.S. Environmental Protection Agency, Washington D.C., September 2002, https://cfpub.epa.gov/ncea/iris/iris_documents/documents/toxreviews/0088tr.pdf. Accessed: Jan 2018.

[10] M. Saraji, M. Marzban, Determination of 11 priority pollutant phenols in wastewater using dispersive liquid—liquid microextraction followed by high-performance liquid chromatography—diode-array detection, Anal. Bioanal. Chem. 396 (2010) 2685–2693.

[11] T. Heberer, H.-J. Stan, Detection of more than 50 substituted phenols as their t-butyldimethylsilyl derivatives using gas chromatography-mass spectrometry, Anal. Chim. Acta 341 (1997) 21-34.

[12] N. Kolahchi, M. Braiek, G. Ebrahimipour, S, O. Ranaei-Siadat, F. Lagarde, N. Jaffrezic-Renault, Direct detection of phenol using a new bacterial strain-based conductometric biosensor, J. Environ. Chem. Eng. 6 (2018) 478–484.

[13] Z. Lin, Y. Xiao, Y. Yin, W. Hu, W. Liu, H. Yang, Facile synthesis of enzyme-inorganic hybrid nanoflowers and its application as a colorimetric platform for visual detection of hydrogen peroxide and phenol, ACS Appl. Mater. Interfaces 6 (2014) 10775–10782.

[14] V. K. Gupta, H. Karimi-Maleh, R. Sadegh, Simultaneous Determination of Hydroxylamine, Phenol and Sulfite in Water and Waste Water Samples Using A Voltammetric Nanosensor, Int. J. Electrochem. Sci, 10 (2015) 303-316.

[15] W. Lu, G. G. Wallace, M. D. Imisides, Development of conducting polymer modified electrodes for the detection of phenol, Electroanalysis 14 (2002) 325-332.

[16] H. Karimi-Maleh, M. Moazampour, A. A. Ensafi, S. Mallakpour, M. Hatami, Environ. Sci. Pollut. R. 21 (2014), 5879–5888.

[17] S. Yang, J. Liang, S. Luo, C. Liu, Y. Tang, Supersensitive detection of chlorinated phenols by multiple amplification electrochemiluminescence sensing based on carbon quantum dots/graphene, Anal. Chem. 85 (2013) 7720–7725.

[18] P. M. Reddya, S Hsieh, C. Chang, J. Kang, Detection of cyanide ions in aqueous solutions using cost effective colorimetric sensor, J. Hazard. Mater. 334 (2017) 93– 103.

[19] V. K. Gupta, N. Mergu, L. K. Kumawat, A. K. Singh, A reversible fluorescence "off–on–off" sensor for sequential detection of aluminum and acetate/fluoride ions, Talanta 144 (2015) 80–89.

[20] V. K. Gupta, N. Mergu, L. K. Kumawat, A. K. Singh, Selective naked-eye detection of Magnesium (II) ions using acoumarin-derived fluorescent probe, Sens. Actuators B Chem. 207 (2015) 216–223.

[21] V. K. Gupta, A. K. Singh, L. K. Kumawat, Thiazole Schiff base turn-on fluorescent chemosensor for Al3+ion, Sens. Actuators B Chem. 195 (2014) 98–108.

[22] W. Lu, X. Dong, L. Qiu, Z. Yan, Z. Meng, M. Xue, X. He, X. Liu, Colorimetric sensor arrays based on pattern recognition for the detection of nitroaromatic molecules, J. Hazard. Mater. 326 (2017) 130– 137.

[23] L. Hu, X. Yan, Q. Li, X. Zhang, D. Shan, Br-PADAP embedded in cellulose acetate electrospun nanofibers: Colorimetric sensor strips for visual uranyl recognition, J. Hazard. Mater. 329 (2017) 205– 210.

[24] A. Promchat, P. Rashatasakhon, M. Sukwattanasinitt, A novel indolium salt as a highly sensitive and selective fluorescent sensor for cyanide detection in water, J. Hazard. Mater. 329 (2017) 255– 261.

[25] W. Smith, C. E. Waring, An Improved Method for the Preparation of Benzenediazonium Salts, J. Am. Chem. Soc. 64 (2) (1942) 469–470.

[26] D. F. DeTar, M. N. Turetzky, The Mechanisms of Diazonium Salt Reactions. I. The Products of the Reactions of Benzenediazonium Salts with Methanol, J. Am. Chem. Soc. 77, 7 (1955) 1745-1750.

[27] D. F. DeTar, A. R.Ballentine, The Mechanisms of Diazonium Salt Reactions. II. A Redetermination of the Rates of the Thermal Decomposition of Six Diazonium Salts in Aqueous Solution, J. Am. Chem. Soc. 78, 16 (1956) 3916–3920.

[28] D. F. DeTar, M. N. Turetzky, The Mechanisms of Diazonium Salt Reactions. IV. A Kinetic Study of the Reactions of Benzenediazonium Fluoborate with Methanol in the Absence of Oxygen, J. Am. Chem. Soc. 78, 16 (1956) 3925–3928.

[29] S. Vallejos, A. Muñoz, S. Ibeas, F. Serna, F.C. García, J.M. García, Solid sensory polymer substrates for the quantification of iron in blood, wine and water by a scalable RGB technique, J. Mater. Chem. A 1 (2013) 15435-15441.

[30] S. Vallejos, J. A, Reglero, F. C. García, J. M. García, Direct visual detection and quantification of mercury in fresh fish meat using facilely prepared polymeric sensory labels, J. Mater. Chem. A 5 (2017) 13710-13716.

[31] M. Yin, Y. Ye, M. Sun, N. Kang, W. Yang, Facile One-Pot Synthesis of a Polyvinylpyrrolidone-Based Self-Crosslinked Fluorescent Film, Macromol. Rapid Commun. 34 (2013) 616−620.

[32] J. C. Colbert, R. M. Lacy, The effect of substituent groups upon the course of the condensation reaction between benzenediazonium salts and phenols, J. Am. Chem. Soc. 68 (1946) 270-271.

[33] E. S. Lewis, E. B. Miller, The effect of structure of the alkyl group on the rates of decomposition of alkyl substituted benzenediazonium salts, J. Am. Chem. Soc. 75 (1953) 429-432.

[34] J. M. García, S. Vallejos, E. Hernando, M. Trigo-López, F. C. García, M. Garcia-Valverde, D. I. Iturbe, M. J. Cabero, R. Quesada, Polymeric chemosensor for the detection and quantification of chloride in human sweat. Application to the diagnosis of cystic fibrosis, J. Mater. Chem. B (2018) DOI: 10.1039/C8TB00682B.

[35] S. Vallejos, A. Muñoz, F. García, F. Serna, S. Ibeas, J. M. García, Methacrylate copolymers with pendant piperazinedione-sensing motifs as fluorescent chemosensory materials for the detection of Cr(VI) in aqueous media, J. Hazard. Mater. 227– 228 (2012) 480– 483.

[36] S. E. Bustamante, B L. Rivas, J. M. García, S. Vallejos, F. García, Synthesis of a polymeric sensor containing an occluded pyrylium salt and its application in the colorimetric detection of trimethylamine vapors, J. Appl. Polym. Sci. 2018, DOI: 10.1002/APP.46185.

[37] Y. C. Fiamegos, C. D. Stalikas, G. A. Pilidis, M. I. Karayannis, Synthesis and analytical applications of 4-aminopyrazolone derivatives as chromogenic agents for the spectrophotometric determination of phenols, Anal. Chim. Acta 403 (2000), 315-323.

[38] Y. Jyisy, C. Ming-Liang, Development of an SPME/ATR-IR chemical sensor for detection of phenol type compounds in aqueous solutions, Analyst 126 (2000) 881-886.

[39] L. Fariña, E. Boido, F. Carrau, E. Dellacassa, Determination of volatile phenols in red wines by dispersive liquid–liquid microextraction and gas chromatography–mass spectrometry detection, J. Chromatogr. A 1157 (2007) 46-50.

[40] C. Pérez Lamela, J. Simal Lozano, P. Paseiro Losada, S. Paz Abuín, J. Simal Gándara,Simultaneous determination of phenol, formaldehyde and benzyl alcohol in Mannich products used as curing agents for epoxy resins by direct gas chromatographic-FID analysis, Analysis 21 (1993) 367-371.

[41] A. Danhel, K. Keung Shiu, B. Yosypchuk, J. Barek, K. Peckova, V. Vyskocil, The use of silver solid amalgam working electrode for determination of nitrophenols by HPLC with electrochemical detection, Electroanalysis 21 (2009) 303-308.

[42] W. Markowski, L. K. Czapinska, A. J. Józefczyk, K. Glowniak, Separation and identification of phenolic acids from some species of the asteraceae family using HPLC with a diode array detector, J. Liq. Chromatogr. Relat. Technol. 21 (1998) 2497-2507.

[43] Q. Wang, H. Qiu, J. Li, X. Liu, S. Jiang, On-line coupling of ionic liquid-based single-drop microextraction with capillary electrophoresis for sensitive detection of phenols, J. Chromatogr. A 1217 (2010) 5434-5439.

[44] Reregistration Eligibility Decision (RED) m-cresol and xylenol https://archive.epa.gov/pesticides/reregistration/web/pdf/4027.pdf (accessed Mar 20, 2018).

[45] Pesticide fact sheet-Fenhexamid https://www3.epa.gov/pesticides/chem_search/reg_actions/registration/fs_PC-090209_20-May-99.pdf (accessed Mar 20, 2018).

[46] S. Tayama, N. Kamiya and Y. Nakagawa, Genotoxic effects of o-phenylphenol metabolites in CHO-K1 cells, Mutat. Res. Genet. Toxicol. Environ. Mutagen. 223 (1989) 23-33.

[47] R. Maggio, P. Damiani, A. Olivieri, Four-way kinetic-excitation-emission fluorescence data processed by multi-way algorithms. Determination of carbaryl and 1-naphthol in water samples in the presence of fluorescent interferents, Anal. Chim. Acta, 677 (2010) 97-107.

[48] H. Sun, O. Shen, X. Xu, L. Song, X. Wang, Carbaryl, 1-naphthol and 2-naphthol inhibit the beta-1 thyroid hormone receptor-mediated transcription in vitro, Toxicology 249 (2008) 238-242.

[49] L. Sendelbach, A review of the toxicity and carcinogenicity of anthraquinone derivatives, Toxicology 57 (1989) 227-240.

[50] Guidelines for drinking-water quality; WHO: Geneva, 1998.

[51] N. Fattahi, Y. Assadi, M. Hosseini, E. Jahromi, Determination of chlorophenols in water samples using simultaneous dispersive liquid–liquid microextraction and derivatization followed by gas chromatography-electron-capture detection, J. Chromatogr. A 1157 (2007) 23-29.

[52] G. Ahmed, R. Laíño, J. Calzón, M. García, Facile synthesis of water-soluble carbon nano-onions under alkaline conditions, Microchim. Acta 182 (2014) 51-59.

[53] L. Vandenberg, R. Hauser, M. Marcus, N. Olea, W. Welshons, Human exposure to bisphenol A (BPA), Reprod. Toxicol. 24 (2007) 139-177.

Table 1 Comparative table of different phenol analytical methods.

Sensor	Cost of the analyses/materials	Detection method	Response Time (min)	LOD (ppm)	Naked-eye detection	Ref.
I	High	UV-Vis	5.00	<0.005	Yes	37
II	Low	SPEM/ATR-IR	20.0	<5.47	No	38
III	High	GC–MS	ND	<159	No	39
IV	High	GC-FID	30.0	<50	No	40
V	High	HPLC-ED	6.00	<3.48	No	41
VI	High	HPLC-DAD	9.56	ND	No	42
VII	High	CE	ND	<0.05	No	43
$F_{025}B$	Low	UV-Vis	3.33	0.12[a]	Yes	This work
$F_{025}B$	Low	Digital picture (RGB parameters defining the digital colors)	3.33	0.03[b]	Yes	This work

[a] LOD for 2-phenylphenol.
[b] LOD for *m*-cresol.

Table 2. Tested phenols and their uses.

Phenol derivate	Use	Ref.
2,4-dimethylphenol	Pesticide	44
fenhexamid	Fungicide	45
2-phenylphenol	Fungicide	46
1-naphthol	Derived from the degradation of the pesticide carbaryl.	47,48
1,8-dihydroxyanthraquinone	Pesticide	49
2-chlorophenol	Pesticide	50,51
4-chlorophenol	Pesticide	49,50
2,4-dichlorophenol	Derived from the degradation of the pesticide 2-(2,4-dichlorophenoxy)acetic acid	49,50
2-methyl-4-chlorophenol	Derived from the degradation of the pesticide MCPA	49
2-nitrophenol	Byproduct in the synthesis of pesticides	7
4-nitrophenol	Byproduct in the synthesis of pesticides	52
2,4-dinitrophenol	Byproduct in the synthesis of dyes	7
bisphenol A	Used in polymers for the alimentary industry	53

Table 3. Limit of detection and quantification for phenols, using the sensory materials **F_{005}B** and **F_{025}B,** calculated using UV-Vis analysis and the blue parameter (B) of the digital definition of the color of the films.

Phenol code	Phenol derivative	UV-Vis analysis		RGB analysis	
		LOD	LOQ	LOD	LOQ
A	*m*-cresol	135 ppb	408 ppb	27 ppb	82 ppb
B	2-chlorophenol	366 ppb	1.1 ppm	123 ppb	373 ppb
C	bisphenol-A	217 ppb	657 ppb	221 ppb	670 ppb
D	4-chloro-2-methylphenol	203 ppb	614 ppb	253 ppb	766 ppb
E	2,4-dimethylphenol	151 ppb	457 ppb	300 ppb	910 ppb
F	2-phenylphenol	133 ppb	402 ppb	207 ppb	627 ppb
G	1-naphthol	121 ppb	369 ppb	181 ppb	547 ppb
H	2,4-dinitrophenol	299 ppb	905 ppb	410 ppb	1.2 ppm
I	4-chlorophenol	326 ppb	987 ppb	782 ppb	2.4 ppb
J	1,8-dihydroxyanthraquinone	276 ppb	836 ppb	*1.8 ppm	*5.6 ppm
K	2-nitrophenol	76 ppm	229 ppm	43 ppm	131 ppm
L	fenhexamid	193 ppm	584 ppm	49 ppm	150 ppm
M	2,4-dichlorophenol	38 ppm	85 ppm	80 ppm	242 ppm

*The red component of the RGB parameters was used in this case instead of the blue due to the different color change observed in comparison to the rest of phenols.

Table 4. ICP-MS analysis for the lab-made solution of 2-phenylphenol (0.58 M in aqueous 0.1 M NaOH) and the commercial product.

	Lab-made solution	Commercial product
Si (ppb)	25.7	15080.5
Mn (ppb)	--	1.8
Zn (ppb)	1.2	622.3
Pd (ppb)	0.2	49.4
Ba (ppb)	0.1	7.2